On Shannon's Strategy of Computing Degree Based Entropy Measures for Melamine Cyanuric Acid Molecular Structure

Renai, P. N. A. D.[1], Roy, S. [ID][1], and Husin, M. N.* [ID][2]

[1]*Department of Mathematics, Vellore Institute of Technology, Vellore, India*
[2]*Faculty of Computer Science and Mathematics,*
Universiti Malaysia Terengganu, Terengganu, Malaysia

E-mail: nazri.husin@umt.edu.my
*Corresponding author

Abstract

This manuscript introduces an existing enhanced approach to Shannon's method for computing degree-based entropies, integrating both additive and multiplicative degree-based topological indices. It also assesses the physicochemical correlation capacity of the melamine cyanuric acid molecular structure, addressing implications for physicochemical and biological realms. Graph theoritical computational techniques were applied to investigate the interaction between melamine and cyanuric acid, revealing diverse binding configurations and emphasizing the importance of structural diversity in these complexes. The study represents the melamine cyanuric acid structure using three chemical graphs and establishes a hydrogen-bonded biomolecular network. From the comparison between multiplicative and additive degree based entropy measures the bond additive descriptors showed superior predictive performance for entropies, prompting further analysis on their correlation with entropy measures using linear regression models. Significant relationships between bond additive degree-based descriptors and entropy measures were observed, demonstrating potential for predictive modeling in physicochemical contexts.

Keywords: degree based entropies; edge partition; topological indices; physicochemical properties; melamine cyanuric acid.

P. N. A. D. Renai *et al.*

Malaysian J. Math. Sci. 19(1): 241–267(2025) *241 - 267*

1   Introduction

According to the literature review on supramolecular structures, a discussion on coordination motivated self-assemblies of molecular frameworks has enabled the development of various supramolecular architectures and structures, from straightforward two-dimensional macrocycles to massive, intricate three-dimensional cages [7, 11]. Molecular recognition and the creation of high-order assemblies by non-covalent interactions are the main topics of supramolecular chemistry, also referred to as chemistry beyond the molecule. As a result of this, supramolecular chemistry became a well-known chemistry discipline. Since supramolecular systems are made up of non-covalent interactions, they bind together as building blocks[14]. Molecular interactions, which include a variety of favorable and repulsive connections including hydrogen bonding and metal-ligand interactions, are significant in supramolecular chemistry [23]. In addition, the study explores the variety of molecular interaction, including dendrimer [15], metal-organic framework [16], Corona product, Aluminophosphates [27], chain of diphenylene [20], silicate carbide, nanocones and network. These investigations advance our knowledge of the features and attributes of various substances and materials of interactions. Melamine, a versatile organic base, starts its part as urea. Through a two-step process, urea transforms first into cyanuric acid, then condenses with ammonia to become melamine. Interestingly, this reaction also produces byproducts like cyanuric acid, ammeline, and ammelide. Remarkably, melamine packs a powerful punch in its tiny form, boasting a whopping 66 percent nitrogen by weight. Melamine has been used in a variety of commercial products such as countertops, dry erase boards, fabrics, and flame retardants. Melamine has been used in fertilisers since 1958, and it is occasionally used as a nonprotein nitrogenous source in cow feed. However, because of its slow hydrolysis in ruminants, it was later discovered to be an ineffective nonprotein nitrogen source for animals [13].

For over 60 years, a combination of chemicals has been used in pools to fight the sun's weakening effect on chlorine. This combo, including hypochlorous acid, chlorine, and cyanuric acid derivatives, keeps the disinfectant chlorine active longer, reducing both disinfection failures and the need for constant re-dosing. Additionally, pre-made disinfectants containing cyanuric acid derivatives are readily available. These chemicals and their manufacturing methods are well-understood and established [4, 8]. Upon ingestion, melamine undergoes metabolic breakdown within the body, converting into cyanuric acid, a process that may result in the formation of solid crystals known as MCA melamine-cyanuric acid co-crystals within the kidneys. These crystals have the potential to inflict damage on renal tissue, leading to organ failure. The public's concern regarding the toxicity of melamine has heightened in response to several incidents where unscrupulous suppliers adulterated products like wheat or baby milk with melamine to falsely elevate the protein content [25, 29]. Recent reports from various developing countries have further underscored the prevalence of such deceptive practices [12]. Notably, the crystal morphology of melamine-cyanuric acid differs between samples produced in vitro and those formed in vivo [17, 26]. Melamine, melamine cyanuric acid, and their derivatives find extensive use as flame retardants due to their unique property of releasing nitrogen gas when exposed to heat or flames. In this investigation, we evaluate the entropy values based on degree for three distinct types of MCA growths, providing valuable insights for readers interested in this domain.
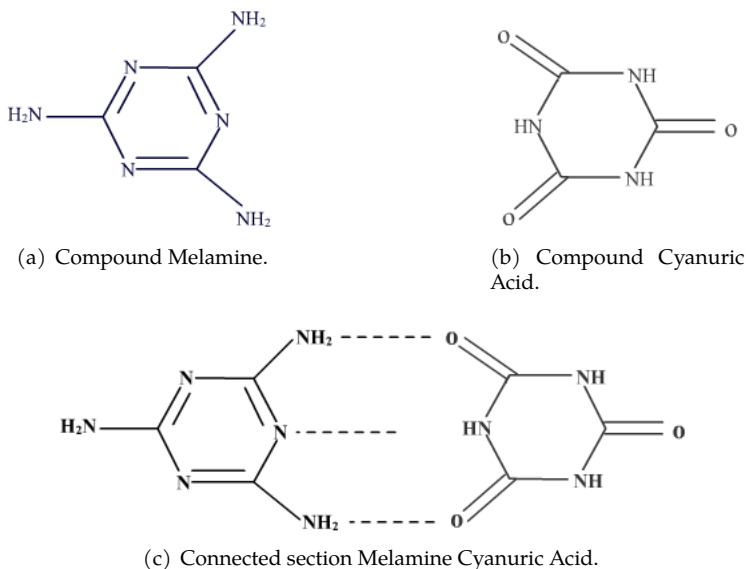
1.1   About the molecular arrangements of MCA

(a) Compound Melamine.

(b) Compound Cyanuric Acid.

(c) Connected section Melamine Cyanuric Acid.

Figure 1: The molecular arrangements of MCA.

A single MCA molecule forms a crystalline structure, comprising a finite arrangement of atoms bonded via hydrogen bonds. This structure arises from a 1:1 stoichiometric combination of melamine (M) and cyanuric acid (CA). To aid in visualization, both atoms and hydrogen bonds can be depicted as vertices and edges in a graph. Notably, the MCA compound exhibits regular hexagonal rings containing either six ($C6$) or eight ($C8$) atoms along its structure, as shown in Figure 1(c) illustrating the initial dimension arrangement. The linear configuration of MCA is denoted as MCA linear tape ($MCA.LT_n$), as depicted in Figure 2. Moreover, the hexagonal Cyclic Rosette Structure (CRS) of MCA, as per [17], is represented as the linear chain CRS ($MCA.LC_n$), with $MCA.LC_4$ illustrated in Figure 3. Similarly, the triangular CRS system is defined as $MCA.T_n$, with $MCA.T_n$ shown in Figure 4. Melamine cyanuric acid is a complex formed by the reaction between melamine and cyanuric acid. Melamine is a nitrogen-rich compound with the molecular formula $C_3H_6N_6$, while cyanuric acid has the formula $C_3H_3N_3O_3$. When these two compounds react, they form a hydrogen-bonded network known as melamine cyanuric acid complex or melamine cyanurate.

The molecular structure of melamine cyanuric acid complex involves multiple hydrogen bonds between melamine and cyanuric acid molecules. Melamine contains three amine groups (-NH$_2$) and three triazine rings, while cyanuric acid contains three carboxylic acid groups (-COOH) and three triazine rings. In the complex structure, the amine groups of melamine form hydrogen bonds with the carboxylic acid groups of cyanuric acid. The specific arrangement of these molecules results in a network-like structure that can be visualized as a repeating pattern of melamine and cyanuric acid units connected through hydrogen bonds. This structure is significant because it plays a role in the stability and properties of the complex. Melamine cyanuric acid complexes have garnered attention due to their involvement in food safety issues. There have been concerns about their potential formation in food products, particularly when melamine is illegally added to food or animal feed to increase apparent protein content. The formation of these complexes can lead to health risks, such as kidney damage, especially in cases of high exposure. Melamine

cyanuric acid (MCA) has been a subject of computational studies due to its relevance in materials science, chemistry, and biology. Here are some key points about computational studies related to MCA:

- Structural Analysis: Computational methods like molecular dynamics simulations and density functional theory (DFT) calculations have been used to study the structural properties of MCA. These techniques help in understanding the arrangement of molecules, intermolecular interactions, and stability of MCA crystals.

- Energetics and Stability: Computational studies can provide insights into the energetics of MCA, including the calculation of binding energies between melamine and cyanuric acid molecules. These calculations help in predicting the stability of MCA complexes and their potential applications in various fields.

- Phase Transitions: Computational modeling can simulate phase transitions in MCA under different conditions such as temperature and pressure. This is important for understanding the thermodynamic behavior of MCA and its phase diagrams.

- Mechanical Properties: Molecular dynamics simulations can be used to investigate the mechanical properties of MCA crystals, such as elastic moduli, hardness, and fracture behavior. These properties are crucial for evaluating the suitability of MCA in structural applications.

- Electronic Structure: DFT calculations can elucidate the electronic structure of MCA, including band structures, density of states, and electronic properties. This information is valuable for understanding the optical, electronic, and magnetic properties of MCA-based materials.

- Adsorption and Catalysis: Computational studies have explored the adsorption properties of MCA for various molecules and pollutants, as well as its catalytic activity in chemical reactions. This has implications for environmental remediation and catalysis research.

- Biological Interactions: In the context of biology, computational methods can simulate the interactions of MCA with biomolecules like proteins and nucleic acids. These studies contribute to understanding the potential biomedical applications of MCA and its derivatives.

- Design of MCA-based Materials: By combining computational predictions with experimental synthesis, researchers can design novel materials based on MCA with tailored properties for specific applications such as sensors, drug delivery systems, and nanocomposites.

Overall, computational studies play a crucial role in unraveling the fundamental properties and potential applications of melamine cyanuric acid, contributing to advancements in materials science, chemistry, and related disciplines [5].

Analyzing the molecular structure of melamine cyanuric acid complexes is crucial for understanding their behavior, properties, and potential health implications. As our contribution, we have utilized a graph theoretical (topological characterization) method to figure out the molecular invariants. In recent years, there has been a surge in the application of these novel chemical compounds, driven by advancements in "topological indices." These indices serve as potent tools for predicting the physicochemical characteristics of diverse compounds, fostering significant breakthroughs [6]. Quantitative structure-property relations (QSPR) and quantitative structure-activity relations (QSAR) represent two prominent applications of topological indices [9, 28]. Due to their structural invariance with respect to molecular graphs and their ability to capture molecular network interconnections, these indices have garnered considerable attention in recent years, particularly in the context of QSPR and QSAR studies [2, 3]. The integration of topological indices with entropy measures holds immense promise for advancing QSPR and QSAR investigations.

Recent research indicates a direct correlation between entropy data and the physical properties of various chemical families, including oxidation states of carbon atoms and rotational symmetry numbers. Motivated by this correlation, we are currently engaged in computing the topological indices and their associated entropy measures for the melamine cyanuric acid (MCA) compound, aiming to uncover its potential future applications [10]. In this paper, we have defined some standard additive and multiplicative version topological indices in Tables 1 and 2 with potential application abilities for some MCA molecular families to predict their physicochemical interactions. They are namely

- **Additive version** the first Zagreb index (M1), second Zagreb Index (M2), the Randic index (R), General Randic index (R_α), the Sum-connectivity index (S1), General Sum-connectivity index (S2), the Geometric arithmetic index (GA), Atom-bond connectivity index (ABC), Harmonic index (H), and Hyper Zagreb index (HM).

- **Multiplicative version** the first multiplicative Zagreb index (MM1), second multiplicative Zagreb Index (MM2), the multiplicative Randic index (MR), multiplicative General Randic index (MR_α), the multiplicative Sum-connectivity index (MS1), multiplicative General Sum-connectivity index (MS2), the multiplicative Geometric arithmetic index (MGA), multiplicative Atom-bond connectivity index (MABC), multiplicative Harmonic index (MH), and multiplicative Hyper Zagreb index (MHM).

The defined topological indices from Tables 1 and 2, numerical descriptors derived from a molecule's configuration. These indices have found broad utility across various domains, encompassing thermodynamics, pharmaceutical exploration and development, and the analysis of QSPR and QSAR. Noteworthy is the substantial correlation established in research between the "atom-bond connectivity index" and pivotal attributes such as boiling points and heats of formation for specific groups of isomeric octanes. This underscores the profound insights that topological indices can furnish regarding diverse molecular attributes [10].

2 Computational Strategies

We initiate our discussion by introducing some fundamental notations that will be employed throughout this manuscript. Let's envision a basic graph, denoted as G, where the nodes symbolize the atoms constituting melamine cynuric acid, and the edges signify the carbon bonds linking them. Here, the symbol d_p signifies the count of atoms directly bonded to a given carbon atom, denoted as vertex p (termed as the degree of vertex p). We define two distinct metrics for every edge, depending on the degrees of its terminal vertices, outlined as follows [1]:

- The metric $x^+(e) = d_p + d_q$ signifies the sum of degrees for vertices p and q, where $e = pq \in E(G)$.

- The metric $x^*(e) = d_p * d_q$ denotes the product of degrees for vertices p and q, where $e = pq \in E(G)$.

Furthermore, using the defined notations and topological indices we compute the indices expressions and the numerical values using the grap theoritical method and followed by that we compute the associated entropy values using Shannon's strategy. A QSPR model (correlation analysis) using the linear regression method has been conducted between the indices and the associated entropy values to determine the goodness of fit. The indices defined in Tables 1 and

Table 1: Additive version of degree-based topological descriptors in QSPR analysis.

Index	Definition & Formula
First Zagreb Index	The sum of the squares of vertex degrees of all edges in the graph. $M_1(G) = \sum\limits_{pq \in E(G)} [x^+(e)]$
Second Zagreb Index	The sum of the product of the vertex degrees of all edges in the graph. $M_2(G) = \sum\limits_{pq \in E(G)} [x^*(e)]$
General Randić Index	The sum of the powers of the product of vertex degrees of all edges in the graph. $R_\alpha(G) = \sum\limits_{pq \in E(G)} [x^*(e)]^\alpha$
Randić Index	The sum of the reciprocal square roots of the product of vertex degrees of all edges in the graph. $R(G) = \sum\limits_{pq \in E(G)} [x^*(e)]^{-\frac{1}{2}}$
Hyper Zagreb Index	The sum of the squares of the squares of vertex degrees of all edges in the graph. $HM(G) = \sum\limits_{pq \in E(G)} [x^+(e)]^2$
Sum Connectivity Index	The sum of reciprocals of square roots of vertex degrees of all edges in the graph. $SCI_1(G) = \sum\limits_{pq \in E(G)} \dfrac{1}{\sqrt{x^+(e)}}$
General Sum Connectivity Index	The sum of powers of vertex degrees of all edges in the graph. $\chi_\alpha(G) = \sum\limits_{pq \in E(G)} [x^+(e)]^\alpha$
Geometric Arithmetic Index	The sum of ratios of twice the square roots of vertex degrees to vertex degrees of all edges in the graph. $GA(G) = \sum\limits_{pq \in E(G)} \dfrac{2\sqrt{x^*(e)}}{x^+(e)}$
Atom Bond Connectivity Index	The sum of square roots of the difference between vertex degrees divided by the product of vertex degrees of all edges in the graph. $ABC(G) = \sum\limits_{pq \in E(G)} \sqrt{\dfrac{x^+(e) - 2}{x^*(e)}}$
Harmonic Index	The sum of reciprocals of vertex degrees of all edges in the graph. $H(G) = \sum\limits_{pq \in E(G)} \dfrac{2}{x^+(e)}$

P. N. A. D. Renai *et al.*

Malaysian J. Math. Sci. 19(1): 241–267(2025) *241 - 267*

Table 2: Multiplicative version of degree-based topological descriptors in QSPR analysis.

Index	Definition & Formula
First Zagreb Index	The product of the squares of vertex degrees of all edges in the graph. $MM_1(G) = \prod\limits_{pq \in E(G)} [x^+(e)]$
Second Zagreb Index	The product of the product of the vertex degrees of all edges in the graph. $MM_2(G) = \prod pq \in E(G)[x^*(e)]$
General Randić Index	The product of the powers of the product of vertex degrees of all edges in the graph. $MR_\alpha(G) = \prod\limits_{pq \in E(G)} [x^*(e)]^\alpha$
Randić Index	The product of the reciprocal square roots of the product of vertex degrees of all edges in the graph. $MR(G) = \prod\limits_{pq \in E(G)} [x^*(e)]^{-\frac{1}{2}}$
Hyper Zagreb Index	The product of the squares of the squares of vertex degrees of all edges in the graph. $MHM(G) = \prod\limits_{pq \in E(G)} [x^+(e)]^2$
Sum Connectivity Index	The product of reciprocals of square roots of vertex degrees of all edges in the graph. $MSCI_1(G) = \prod\limits_{pq \in E(G)} \dfrac{1}{\sqrt{x^+(e)}}$
General Sum Connectivity Index	The product of powers of vertex degrees of all edges in the graph. $M\chi_\alpha(G) = \prod\limits_{pq \in E(G)} [x^+(e)]^\alpha$
Geometric Arithmetic Index	The product of ratios of twice the square roots of vertex degrees to vertex degrees of all edges in the graph. $MGA(G) = \prod\limits_{pq \in E(G)} \dfrac{2\sqrt{x^*(e)}}{x^+(e)}$
Atom Bond Connectivity Index	The product of square roots of the difference between vertex degrees divided by the product of vertex degrees of all edges in the graph. $MABC(G) = \prod\limits_{pq \in E(G)} \sqrt{\dfrac{x^+(e) - 2}{x^*(e)}}$
Harmonic Index	The product of reciprocals of vertex degrees of all edges in the graph. $MH(G) = \prod\limits_{pq \in E(G)} \dfrac{2}{x^+(e)}$

2 are commonly used in graph theory and chemical graph theory to characterize the structural properties of graphs and molecules.
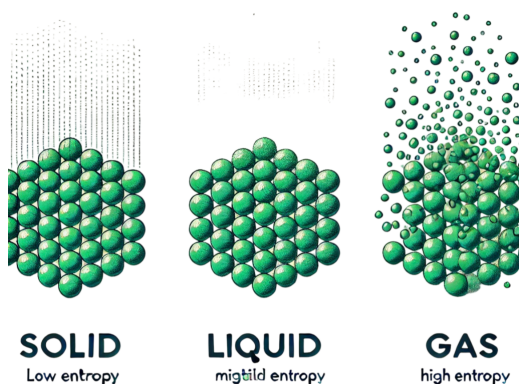
2.1 Entropy

Figure 2: Stages of increasing entropy.

The introduction of the Graph Entropy system, as cited in [21], aimed to characterize the complexity of graphs. Initially developed to represent the challenges in communication and data transmission, this system now finds extensive applications across various sectors, including engineering, biological systems, and physical dissipative structures, among others, as referenced in [18, 24]. There exist two primary types of graph entropies: probabilistic and deterministic. This discussion centers on probabilistic graph entropies due to their widespread use in fields such as communication and chemistry. Among probabilistic graph entropies, two approaches emerge: intrinsic and extrinsic. Intrinsic methodologies segment the graph into sections with similar structures, assigning a probability distribution to each segment. Conversely, extrinsic methodologies incorporate additional information, like node labels or edge weights, to define the probability distribution. For extrinsic metrics, a probability function is allocated to graph elements like vertices or edges. Utilizing an entropy function on this probability distribution function yields the calculated numerical values for probabilistic measurements of graph complexity, as outlined in [21].

While various methodologies estimate probabilistic entropy, we have chosen a method reminiscent of Shannon's prominent strategy for our computations. In information communication and transmission, probability functions are assigned to each unit of information as symbols $x_1, x_2, \ldots, x_n$, and Shannon's fundamental informational entropy (h) measure is defined as:

$$h = \sum_{i=1}^{n} p_i \log(p_i)$$

Here, $p_i = \dfrac{N_i}{N}$, where N_i denotes the number of occurrences of x_i in the information and N represents the total length of information, as elaborated in [24]. To elucidate a molecule's structure, we assign probabilities to its bonds based on topological descriptors that encapsulate the molecule's atom and bond arrangement. The calculated entropy is then expressed using the topological index

Y, as described in [19, 24], in the following manner:

$$ENT_Y(G) = \log(Y) - \frac{1}{Y} \sum_{pq \in E(G)} f(e) \log f(e)$$

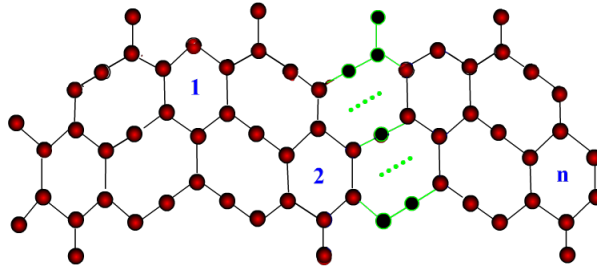## 3 Graph Representation of The Three MCA Structures

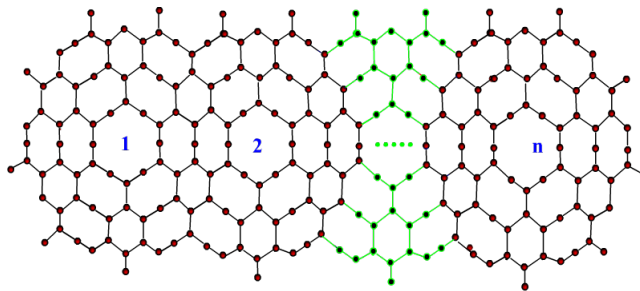Figure 3: Graph view of melamine cyanuric acid linear tape $MCA.LT_n$.

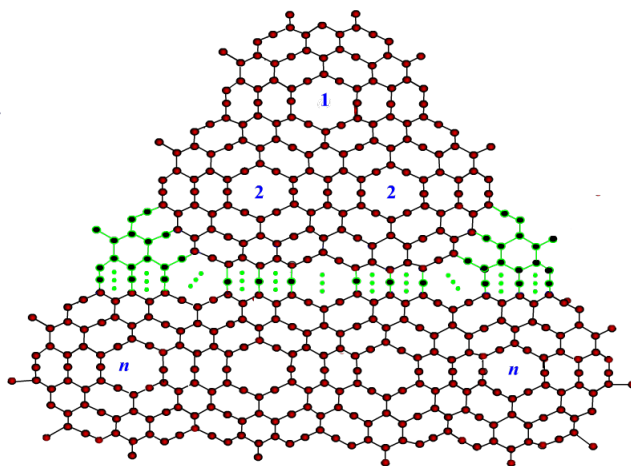Figure 4: Graph view of melamine cyanuric acid linear chain $MCA.LC_n$.

Figure 5: Graph view of melamine cyanuric acid triangular system $MCA.T_n$.

4 Computation of Degree Based Topological Indices of Melamine Cyanuric Acid

Disjoint Edge Partitions for MCA Growth Types: This section begins by outlining the disjoint edge partitions for three distinct types of melamine cyanuric acid (MCA) growths, namely $MCA.LT_n$, $MCA.LC_n$, and $MCA.T_n$. These growth types represent different structural configurations of MCA, each with its unique arrangement of atoms and bonds. $MCA.LT_n$ refers to the linear tape structure of MCA, $MCA.LC_n$ denotes the hexagonal cyclic rosette structure, and $MCA.T_n$ represents the triangular system within MCA. These distinctions are crucial for understanding the diverse molecular arrangements and properties within the MCA compound.

Computing Indices Expressions for MCA Families: By utilizing the descriptors and edge partitions provided in Tables 1 and 2, as well as Tables 3 to 5, we performed computations to derive additive and multiplicative versions of index expressions. These expressions were derived based on the formulations presented in Theorems 4.1 to 4.6, specifically tailored for the three MCA molecular families. The additive and multiplicative indices expressions are mathematical representations that encapsulate key structural and topological information about the MCA molecules. They serve as quantitative measures to characterize and compare the structural features of different MCA growth types, aiding in the understanding of their molecular complexities and behaviors.

Overall, these computations and derivations enhance our understanding of the structural nuances and topological characteristics inherent in various MCA growth types, contributing to a comprehensive analysis of MCA molecular families.

The total number of edges for $MCA.LT_n$ can be expressed as,

$$|E(MCA.LT_n)| = \frac{1}{4}(66n + (-1)^n + 39).$$

For $MCA.LC_n$, the total number of edges is given by,

$$|E(MCA.LC_n)| = 69n + 30.$$

The total number of edges in $MCA.T_n$ is represented as,

$$|E(MCA.T)| = 18n^2 + 66n + 15.$$

Table 3: Edge Partitions of Melamine cyanuric acid $MCA.LT_n$.

Edge Type	$|E_i(MCA.LT_n)|$
(1,3)	$|E_1| = \frac{1}{4}(6n + (-1)^n + 11)$
(2,3)	$|E_2| = \frac{1}{2}(2n + (-1)^n + 7)$
(2,2)	$|E_3| = \frac{1}{2}(14n + (-1)^n + 3)$
(3,3)	$|E_4| = 7n + 2$

Table 4: Edge Partitions of Melamine cyanuric acid $MCA.LC_n$.

Edge Type	$|E_i(MCA.LC_n)|$
(1,3)	$|E_1| = 3n + 6$
(2,3)	$|E_2| = 32n + 10$
(2,2)	$|E_3| = 2n + 4$
(3,3)	$|E_4| = 32n + 10$

Table 5: Edge Partitions of Melamine cyanuric acid $MCA.T_n$.

Edge Type	$|E_i(MCA.T_n)|$
(1,3)	$|E_1| = 3n + 6$
(2,3)	$|E_2| = 9n^2 + 27n + 6$
(2,2)	$|E_3| = 6n$
(3,3)	$|E_4| = 9n^2 + 30n + 3$

4.1   Computation of additive degree based topological indices

Theorem 4.1. *Let $MCA.LT_n$ be the Melamine cyanuric acid linear tape graph with dimension n. Then,*

1. $M_1(MCA.LT_n) = 87n + \dfrac{3(-1)^n}{2} + \dfrac{89}{2}.$

2. $M_2(MCA.LT_n) = 118n + \dfrac{5(-1)^n}{2} + \dfrac{115}{2}.$

3. $R(MCA.LT_n) = \dfrac{35n}{6} + \dfrac{\sqrt{3}((3n)/2 + (-1)^n/4 + 11/4)}{3} + \dfrac{(\sqrt{6}(n + (-1)^n/2 + 7/2))}{6} + \dfrac{(-1)^n}{4} + \dfrac{17}{12}.$

4. $R_\alpha(MCA.LT_n) = 6^\alpha \left(n + \dfrac{(-1)^n}{2} + \dfrac{7}{2} \right) + 9^\alpha(7n + 2) + 4^\alpha \left(7n + \dfrac{(-1)^n}{2} + \dfrac{3}{2} \right) + 3^\alpha \left(\dfrac{3n}{2} + \dfrac{(-1)^n}{4} + \dfrac{11}{4} \right).$

5. $HM(MCA.LT_n) = \left(470n + 17(-1)^n + \dfrac{419}{2} \right).$

6. $SCI_1(MCA.LT_n) = \dfrac{17n}{4} + \sqrt{5}\dfrac{\left(n + \dfrac{(-1)^n}{2} + \dfrac{7}{2} \right)}{5} + \dfrac{3(-1)^n}{8} + \dfrac{(\sqrt{6}(7n + 2))}{6} + \dfrac{17}{8}.$

7. $\chi_\alpha(MCA.LT_n) = 5^\alpha \left(n + \dfrac{(-1)^n}{2} + \dfrac{7}{2} \right) + 6^\alpha(7n + 2) + 4^\alpha \left(7n + \dfrac{(-1)^n}{2} + \dfrac{3}{2} \right) + 4^\alpha \left(\dfrac{3n}{2} + \dfrac{(-1)^n}{4} + \dfrac{11}{4} \right).$

8. $GA(MCA.LT_n) = 8n + \dfrac{\sqrt{3}(6n + (-1)^n + 11)}{8} + \dfrac{\sqrt{6}(14n + (-1)^n + 3)}{5} - \dfrac{(-1)^n}{2} + \dfrac{11}{2}.$

9. $ABC(MCA.LT_n) = \dfrac{14n}{3} + \dfrac{\sqrt{2}(2n + (-1)^n + 7)}{4} + \dfrac{\sqrt{2}(14n + (-1)^n + 3)}{4} + \dfrac{\sqrt{6}(6n + (-1)^n + 11)}{12} + \dfrac{4}{3}.$

10. $H(MCA.LT_n) = \dfrac{179n}{15} + \dfrac{2(-1)^n}{5} + \dfrac{163}{15}.$

Theorem 4.2. *Let $MCA.LC_n$ be the Melamine cyanuric acid linear chain graph with dimension n. Then,*

1. $M_1(MCA.LC_n) = 372n + 150.$

2. $M_2(MCA.LC_n) = 497n + 184.$

3. $R(MCA.LC_n) = \dfrac{35n}{3} + \dfrac{\sqrt{3}(3n+6)}{3} + \dfrac{\sqrt{6}(32n+10)}{6} + \dfrac{16}{3}.$

4. $R_\alpha(MCA.LC_n) = 4^\alpha(2n+4) + 3^\alpha(3n+6) + 6^\alpha(32n+10) + 9^\alpha(32n+10).$

5. $HM(MCA.LC_n) = (2032n + 770).$

6. $SCI_1(MCA.LC_n) = \dfrac{5n}{2} + \dfrac{\sqrt{5}(32n+10)}{5} + \dfrac{\sqrt{6}(32n+10)}{6} + 5.$

7. $\chi_\alpha(MCA.LC_n) = 4^\alpha(2n+4) + 4^\alpha(3n+6) + 5^\alpha(32n+10) + 6^\alpha(32n+10).$

8. $GA(MCA.LC_n) = 34n + \dfrac{\sqrt{3}(3n+6)}{2} + \dfrac{2\sqrt{6}(32n+10)}{5} + 14.$

9. $ABC(MCA.LC_n) = \dfrac{64n}{3} + \dfrac{\sqrt{2}(2n+4)}{2} + \dfrac{\sqrt{2}(32n+10)}{2} + \dfrac{\sqrt{2}\sqrt{3}(3n+6)}{3} + \dfrac{20}{3}.$

10. $H(MCA.LC_n) = \dfrac{779n}{30} + \dfrac{37}{3}.$

Theorem 4.3. *Let $MCA.T_n$ be the Melamine cyanuric acid Triangular system graph with dimension n. Then,*

1. $M_1(MCA.T_n) = 99n^2 + 351n + 72.$

2. $M_2(MCA.T_n) = 135n^2 + 465n + 81.$

3. $R(MCA.T_n) = 13n + \dfrac{\sqrt{6}(9n^2+27n+6)}{6} + 3n^2 + \dfrac{\sqrt{3}(3n+6)}{3} + 1.$

4. $R_\alpha(MCA.T_n) = 3^\alpha(3n+6) + 6^\alpha(9n^2+27n+6) + 4^\alpha(6n) + 9^\alpha(9n^2+30n+3).$

5. $HM(MCA.T_n) = (549n^2 + 1899n + 354).$

6. $SCI_1(MCA.T_n) = \dfrac{9n}{2} + \dfrac{\sqrt{5}(9n^2+27n+6)}{5} + \dfrac{\sqrt{6}(9n^2+30n+3)}{6} + 3.$

7. $\chi_\alpha(MCA.T_n) = 4^\alpha(3n+6) + 5^\alpha(9n^2+27n+6) + 4^\alpha(6n) + 6^\alpha(9n^2+30n+3).$

8. $GA(MCA.T_n) = 36n + \dfrac{2\sqrt{6}(9n^2+27n+6)}{5} + \dfrac{\sqrt{6}(3n+6)}{2} + 3.$

9. $ABC(MCA.T_n) = 20n + \dfrac{\sqrt{2}(9n^2+27n+6)}{2} + 3\sqrt{2}n + 6n^2 + \dfrac{\sqrt{2}\sqrt{3}(3n+6)}{3} + 2.$

10. $H(MCA.T_n) = \dfrac{33n^2}{5} + \dfrac{253n}{10} + \dfrac{32}{5}.$

Example

1.
$$M_1(G) = \sum_{pq \in E(G)} [x^+(e)]$$

$$
\begin{aligned}
M_1(MCA.LT_n) =& (1+3)(3n+6) + (2+3)(9n^2 + 27n + 6) + (2+2)(6n) + \\
& (3+3)(9n^2 + 27n + 3)77 \\
=& 99n^2 + 351n + 72.
\end{aligned}
$$

2.
$$M_2(G) = \sum_{pq \in E(G)} [x^*(e)]$$

$$
\begin{aligned}
M_2(MCA.LT_n) =& (1 \times 3)(3n+6) + (2 \times 3)(9n^2 + 27n + 6) + (2 \times 2)(6n) + \\
& (3 \times 3)(9n^2 + 27n + 3) \\
=& 497n + 184.
\end{aligned}
$$

3.
$$R_\alpha(G) = \sum_{pq \in E(G)} [x^*(e)]^\alpha$$

$$
\begin{aligned}
R(MCA.LT_n) =& \frac{1}{\sqrt{1 \times 3}}(3n+6) + \frac{1}{\sqrt{2 \times 3}}(9n^2 + 27n + 6) + \frac{1}{\sqrt{2 \times 2}}(6n) + \\
& \frac{1}{\sqrt{3 \times 2}}(9n^2 + 27n + 3) \\
=& 3^\alpha(3n+6) + 6^\alpha(9n^2 + 27n + 6) + 4^\alpha(6n) + 9^\alpha(9n^2 + 30n + 3).
\end{aligned}
$$

4.2 Computation of multiplicative degree based topological indices

Theorem 4.4. *Let $MCA.LT_n$ be the Melamine cyanuric acid linear tape graph with dimwsion n. Then,*

1. $MM_1(MCA.LT_n) = 4^{7n+(-1)^n/2+3/2} * 4^{(3*n)/2+(-1)^n/4+11/4} * 5^{n+(-1)^n/2+7/2} * 6^{7*n+2}.$

2. $MM_2(MCA.LT_n) = 3^{(3*n)/2+(-1)^n/4+11/4} * 4^{7*n+(-1)^n/2+3/2} * 6^{n+(-1)^n/2+7/2} * 9^{7*n+2}.$

3. $MR(MCA.LT_n) = (1/18)^{7*n+2} * (1/12)^{n+(-1)^n/2+7/2} * (1/8)^{7*n+(-1)^n/2+3/2}$
   $* (1/6)^{(3*n)/2+(-1)^n/4+11/4}.$

4. $MR_\alpha(MCA.LT_n) = (1/18)^{7*n+2} * (1/12)^{n+(-1)^n/2+7/2} * (1/8)^{7*n+(-1)^n/2+3/2}$
   $* (1/6)^{(3*n)/2+(-1)^n/4+11/4}.$

5. $MHM(MCA.LT_n) = 16^{7*n+(-1)^n/2+3/2} * 16^{(3*n)/2+(-1)^n/4+11/4} * 25^{n+(-1)^n/2+7/2} * 36^{7*n+2}.$

6. $MSCI_1(MCA.LT_n) = (1/12)^{7*n+2} * (1/10)^{n+(-1)^n/2+7/2}$
   $* (1/8)^{7*n+(-1)^n/2+3/2} * (1/8)^{(3*n)/2+(-1)^n/4+11/4}.$

7. $M\chi_\alpha(MCA.LT_n) = (1/12)^{7*n+2} * (1/10)^{n+(-1)^n/2+7/2} * (1/8)^{7*n+(-1)^n/2+3/2}$
   $* (1/8)^{(3*n)/2+(-1)^n/4+11/4}.$

8. $MGA(MCA.LT_n) = (\sqrt{3}/2)^{(3*n)/2+(-1)^n/4+11/4} * ((2*\sqrt{6})/5)^{n+(-1)^n/2+7/2}.$

9. $MABC(MCA.LT_n) = (2/3)^{7*n+2} * (\sqrt{2}/2)^{n+(-1)^n/2+7/2} * (\sqrt{2}/2)^{7*n+(-1)^n/2+3/2} *$
   $((\sqrt{2}\sqrt{3})/3)^{(3*n)/2+(-1)^n/4+11/4}.$

10. $MH(MCA.LT_n) = (1/3)^{7*n+2} * (2/5)^{n+(-1)^n/2+7/2} * (1/2)^{7*n+(-1)^n/2+3/2}$
    $* (1/2)^{(3*n)/2+(-1)^n/4+11/4}.$

Theorem 4.5. *Let $MCA.LC_n$ be the Melamine cyanuric acid linear chain graph with dimwsion n. Then,*

1. $MM_1(MCA.LC_n) = 4^{2*n+4} * 4^{3*n+6} * 5^{32*n+10} * 6^{32*n+10}$.

2. $MM_2(MCA.LC_n) = 3^{3*n+6} * 4^{2*n+4} * 6^{32*n+10} * 9^{32*n+10}$.

3. $MR(MCA.LC_n) \ = (1/18)^{32*n+10} * (1/12)^{32*n+10} * (1/8)^{2*n+4} * (1/6)^{3*n+6}$.

4. $MR_\alpha(MCA.LC_n) \ = (1/18)^{32*n+10} * (1/12)^{32*n+10} * (1/8)^{2*n+4} * (1/6)^{3*n+6}$.

5. $MHM(MCA.LC_n) \ = 16^{2*n+4} * 16^{3*n+6} * 25^{32*n+10} * 36^{32*n+10}$.

6. $MSCI_1(MCA.LC_n) = (1/12)^{32*n+10} * (1/10)^{32*n+10} * (1/8)^{2*n+4} * (1/8)^{3*n+6}$.

7. $M\chi_\alpha(MCA.LC_n) = (1/12)^{32*n+10} * (1/10)^{32*n+10} * (1/8)^{2*n+4} * (1/8)^{3*n+6}$.

8. $MGA(MCA.LC_n) = (\sqrt{3}/2)^{3*n+6} * ((2*\sqrt{6})/5)^{32*n+10}$.

9. $MABC(MCA.LC_n) = 2^{3*n+6} * 2^{32*n+10} * (\sqrt{2})^{2*n+4} * ((\sqrt{2}*\sqrt{7})/2)^{32*n+10}$.

10. $MH(MCA.LC_n) = (1/3)^{32*n+10} * (2/5)^{32*n+10} * (1/2)^{2*n+4} * (1/2)^{3*n+6}$.

Theorem 4.6. *Let $MCA.T_n$ be the Melamine cyanuric acid Triangular system graph with dimwsion n. Then,*

1. $MM_1(MCA.T_n) = 4^{6*n} * 4^{3*n+6} * 5^{9*n^2+27*n+6} * 6^{9*n^2+30*n+3}$.

2. $MM_2(MCA.T_n) = 3^{3*n+6} * 4^{6*n} * 6^{9*n^2+27*n+6} * 9^{9*n^2+30*n+3}$.

3. $MR(MCA.T_n) \ = (1/18)^{9*n^2+30*n+3} * (1/12)^{9*n^2+27*n+6} * (1/8)^{6*n} * (1/6)^{3*n+6}$.

4. $MR_\alpha(MCA.T_n) \ = (1/18)^{9*n^2+30*n+3} * (1/12)^{9*n^2+27*n+6} * (1/8)^{6*n} * (1/6)^{3*n+6}$.

5. $MHM(MCA.T_n) \ = 16^{6*n} * 16^{3*n+6} * 25^{9*n^2+27*n+6} * 36^{9*n^2+30*n+3}$.

6. $MSCI_1(MCA.T_n) = (1/12)^{9*n^2+30*n+3} * (1/10)^{9*n^2+27*n+6} * (1/8)^{6*n} * (1/8)^{3*n+6}$.

7. $M\chi_\alpha(MCA.T_n) = (1/12)^{9*n^2+30*n+3} * (1/10)^{9*n^2+27*n+6} * (1/8)^{6*n} * (1/8)^{3*n+6}$.

8. $MGA(MCA.T_n) = (2/3)^{9*n^2+30*n+3} * (\sqrt{3}/2)^{3*n+6} * ((2*\sqrt{6})/5)^{9*n^2+27*n+6}$.

9. $MABC(MCA.T_n) = (2/3)^{9*n^2+30*n+3} * (\sqrt{2}/2)^{9*n^2+27*n+6} * (\sqrt{2}/2)^{6*n} * ((\sqrt{2}*\sqrt{3})/3)^{3*n+6}$.

10. $MH(MCA.T_n) = (1/3)^{9*n^2+30*n+3} * (2/5)^{9*n^2+27*n+6} * (1/2)^{6*n} * (1/2)^{3*n+6}$.

Example

1.
$$M_1(G) = \prod_{pq \in E(G)} [x^+(e)]$$

$$MM_1(MCA.LT_n) = (1+3)^{(3n+6)} + (2+3)^{(9n^2+27n+6)} + (2+2)^{(6n)+}$$
$$(3+3)^{(9n^2+27n+3)}$$
$$= 4^{6*n} * 4^{3*n+6} * 5^{9*n^2+27*n+6} * 6^{9*n^2+30*n+3}.$$

2.
$$M_2(G) = \prod_{pq \in E(G)} [x^*(e)]$$

$$\begin{aligned} MM_2(MCA.LT_n) =& (1 \times 3)^{(3n+6)} + (2 \times 3)^{(9n^2+27n+3)} + (2 \times 2)^{(6n)} + \\ & (3 \times 3)^{(9n^2+27n+3)} \\ =& 3^{3*n+6} * 4^{6*n} * 6^{9*n^2+27*n+6} * 9^{9*n^2+30*n+3}. \end{aligned}$$

3.
$$R_\alpha(G) = \prod_{pq \in E(G)} [x^*(e)]^\alpha$$

$$\begin{aligned} MR(MCA.LT_n) =& \frac{1}{\sqrt{1 \times 3}}^{(3n+6)} + \frac{1}{\sqrt{2 \times 3}}^{(9*n^2+27*n+6)} + \frac{1}{\sqrt{2 \times 2}}^{(6n)} + \\ & \frac{1}{\sqrt{3 \times 2}}^{(9*n^2+27*n+3)} \\ =& (1/18)^{9*n^2+30*n+3} * (1/12)^{9*n^2+27*n+6} * (1/8)^{6*n} * (1/6)^{3*n+6}. \end{aligned}$$

5   Computer Based Strategies For Computing Degree Based Numerical Entropy Values

This section utilizes Shannon's entropy to measure the distribution of degree-based topological descriptors, accomplishing this through the establishment of a probability function derived from these descriptors, followed by the application of Shannon's formula for computing the entropy value.

In computing the entropies of melamine cyanuric acid (MCA), we employ equation 2 along with the Hyper Zagreb index, employing this method to ascertain the entropy values associated with the aforementioned index.

Assuming G represents the melamine cyanuric acid linear chain $MCA.LC_n$, the process of calculating the entropy values for both additive and multiplicative degree-based Hyper Zagreb Indices using equation 2 is further expounded below [22].

Additive degree based entropy

$$ENT_{HM}(G) = \log(HM(G)) - \frac{1}{HM(G)} \sum_{pq \in E(G)} [x^+(e)]^2 \log[x^+(e)]^2.$$

Now by substituting the edge partitions from Tables 3 to 5 we get,

$$ENT_{HM}(G) = \log(HM(G)) - \frac{1}{HM(G)}[(3n+6)[1+3]^2\log[1+3]^2 + (32n+10)[2+3]^2\log[2+3]^2$$
$$+ (2n+4)[2+2]^2\log[2+2]^2 + (32n+10)[3+3]^2\log[3+3]^2.$$

$$ENT_{HM}(G) = \log(2032n+770)\frac{\left(\dfrac{989120744954581143n}{140737488355328} + \dfrac{14471128046188807295}{562949953421312}\right)}{(2032n+770)}.$$

Multiplicative degree based entropy

$$ENT_{HM}(G) = \log(HM(G)) - \frac{1}{HM(G)}\prod_{pq\in E(G)}[x^+(e)]^2\log[x^+(e)]^2.$$

Now by substituting the edge partitions from Tables 3 to 5 we get,

$$ENT_{HM}(G) = \log(HM(G)) - \frac{1}{HM(G)}[(3n+6)[1+3]^2\log[1+3]^2 * (32n+10)[2+3]^2\log[2+3]^2$$
$$* (2n+4)[2+2]^2\log[2+2]^2 * (32n+10)[3+3]^2\log[3+3]^2.$$

$$ENT_{HM}(G) = \log(2032n+770) - log((1/3)^{(9*n^2+30*n+3)} * (2/5)^{(9*n^2+27*n+6)} * (1/2)^{(6*n)} *$$
$$(1/2)^{(3*n+6)}) - (18729944304496077/(1/3)^{(9*n^2+30*n+3)}/(2/5)^{(9*n^2+27*n+6)}/$$
$$(1/2)^{(6*n)}/(1/2)^{(3*n+6)} * n * ((18729944304496077 * n)/18014398509481984+$$
$$18729944304496077/9007199254740992)*$$
$$((74278918775366703 * n^2)/22517998136852480+$$
$$(222836756326100109 * n)/22517998136852480+$$
$$24759639591788901/11258999068426240)*$$
$$((14843129681611041 * n^2)/4503599627370496+$$
$$(24738549469351735 * n)/2251799813685248+$$
$$4947709893870347/4503599627370496))/9007199254740992.$$

The derivation of a general entropy expression using Shannon's approach for the three MCA compounds would be quite lengthy if explained as Theorems. However, concerning every topological descriptor, one can simply apply the aforementioned strategy to compute entropy.

Below, in Tables 6, 7, and 8 we have the computed different additive degree based numerical entropy values and in Tables 9, 10, and 11 we have the computed different multiplicative degree based numerical entropy values.

By examining Tables 6 through 11, we have compared and evaluated the performance of multiplicative and additive entropy measures in predicting entropies. The results consistently show that bond-additive descriptors outperform multiplicative ones in this context. To visually demonstrate this trend, Figures 5 and 6 display the entropy values calculated using the additive degree-based approach.

The graphical representations provided for the three distinct MCA structures illustrate the discussed concepts further, enhancing understanding.

6 Additive Degree Based Numerical Entropy Values

Table 6: Additive degree based numerical entropy computation for $MCA.LT_n$.

n	EM_1	EM_2	ER	ER_α	EHM	$ESCI_1$	$E\chi_\alpha$	EGA	$EABC$	EH
1	3.2442	3.3909	3.2375	3.2375	3.2545	3.2545	3.1691	3.2569	3.2558	3.5263
2	3.7493	3.8799	3.7416	3.7416	3.7580	3.7580	3.7702	3.7601	3.7590	4.0013
3	4.0659	4.1721	4.0588	4.0588	4.0744	4.0744	4.0354	4.0766	4.0755	4.2956
4	4.3199	4.4266	4.3124	4.3124	4.3278	4.3278	4.3325	4.3298	4.3287	4.5441
5	4.5110	4.6064	4.5039	4.5039	4.5189	4.5189	4.4926	4.5209	4.5199	4.7256
6	4.6809	4.7784	4.6737	4.6737	4.6885	4.6885	4.6905	4.6905	4.6894	4.8941
7	4.8179	4.9083	4.8109	4.8109	4.8255	4.8255	4.8052	4.8275	4.8265	5.0254
8	4.9457	5.0383	4.9385	4.9385	4.9531	4.9531	4.9536	4.9550	4.9540	5.1529
9	5.0524	5.1399	5.0454	5.0454	5.0598	5.0598	5.0429	5.0618	5.0608	5.2558
10	5.1548	5.2444	5.1477	5.1477	5.1621	5.1621	5.1617	5.1640	5.1629	5.3584

Table 7: Additive degree based numerical entropy computation for $MCA.LC_n$.

n	EM_1	EM_2	ER	ER_α	EHM	$ESCI_1$	$E\chi_\alpha$	EGA	$EABC$	EH
1	4.5859	4.5485	4.5791	4.5791	4.5926	4.5926	4.5124	4.2671	4.9861	4.5847
2	4.5859	4.5485	4.5791	4.5791	4.5926	4.5926	4.5124	4.2671	4.9861	4.5847
3	5.4602	5.4292	5.4547	5.4547	5.4659	5.4659	5.3891	5.1384	5.9024	5.4592
4	5.7160	5.6869	5.7107	5.7107	5.7215	5.7215	5.6453	5.3936	6.1647	5.7150
5	5.9195	5.8901	5.9144	5.9144	5.9249	5.9249	5.8490	5.5968	6.3724	5.9185
6	6.0885	6.0596	6.0835	6.0835	6.0938	6.0938	6.0182	5.7656	6.5442	6.0875
7	6.2330	6.2045	6.2281	6.2281	6.2383	6.2383	6.1629	5.9099	6.6908	6.2321
8	6.3593	6.3310	6.3544	6.3544	6.3645	6.3645	6.2892	6.0361	6.8187	6.3583
9	6.4713	6.4433	6.4665	6.4665	6.4765	6.4765	6.4014	6.1481	6.9320	6.4704
10	6.5721	6.5442	6.5674	6.5674	6.5773	6.5773	6.5022	6.2488	7.0338	6.5712

Table 8: Additive degree based numerical entropy computation for $MCA.T_n$.

n	EM_1	EM_2	ER	ER_α	EHM	$ESCI_1$	$E\chi_\alpha$	EGA	$EABC$	EH
1	4.5859	4.5485	4.5791	4.5791	4.5926	4.5926	4.5670	3.9532	4.5934	4.5847
2	5.3811	5.3506	5.3760	5.3760	5.3869	5.3869	5.3593	4.5904	5.3878	5.3800
3	5.9196	5.3506	5.9155	5.9155	5.9249	5.9249	5.8997	5.0179	5.9259	5.9186
4	6.3335	6.3083	6.3299	6.3299	6.3385	6.3385	6.3148	5.3464	6.3394	6.3327
5	6.6719	6.6479	6.6686	6.6686	6.6766	6.6766	6.6540	5.6165	6.6775	6.6711
6	6.9589	6.9359	6.9559	6.9559	6.9634	6.9634	6.9461	5.8473	6.9643	6.9581
7	7.2085	7.1863	7.2057	7.2057	7.2129	7.2129	7.1918	6.0499	7.2138	7.2078
8	7.4296	7.4080	7.4270	7.4270	7.4339	7.4339	7.4133	6.2309	7.4347	7.4290
9	7.6282	7.6071	7.6257	7.6257	7.6323	7.6323	7.6122	6.3949	7.6332	7.6276
10	7.8084	7.7878	7.8061	7.8061	7.8125	7.8125	7.7928	6.5451	7.8133	7.8079

7 Multiplicative Degree Based Numerical Entropy Values

Table 9: Multiplicative degree based numerical entropy computation for $MCA.LT_n$.

n	EM_1	EM_2	ER	ER_α	EHM	$ESCI_1$	$E\chi_\alpha$	EGA	$EABC$	EH
1	0.5859	0.5485	0.5791	0.5791	0.5926	1.5926	1.5124	1.2671	1.9861	1.1847
2	0.5859	0.5485	0.5791	0.5791	1.5926	1.5926	1.5124	1.2671	2.9861	2.5847
3	0.4602	0.4292	0.4547	0.4547	0.4659	0.4659	0.3891	0.1384	0.9024	1.4592
4	0.4602	0.4292	0.4547	0.4547	0.4659	0.4659	0.3891	0.1384	0.9024	1.4592
5	77.0	135.0	178.6	236.7	280.3	338.3	382.0	440.0	483.6	541.7
6	0.0885	0.0596	0.0835	0.0835	0.0938	0.0938	0.0182	0.7656	1.5442	1.0875
7	0.0885	0.0596	0.0835	0.0835	0.0938	0.0938	0.0182	0.7656	1.5442	1.0875
8	0.3842	1.12	1.62	3.53	4.47	8.55	11.10	18.4	23.1	37.1
9	0.4713	0.4433	0.4665	0.4665	0.4765	0.4765	0.4014	2.1481	3.9320	4.4704
10	0.5721	0.5442	0.5674	0.5674	0.5773	0.5773	1.5022	2.2488	2.0338	2.5712

Table 10: Multiplicative degree based numerical entropy computation for $MCA.LC_n$.

n	EM_1	EM_2	ER	ER_α	EHM	$ESCI_1$	$E\chi_\alpha$	EGA	$EABC$	EH
1	0.2442	0.3909	0.2375	0.2375	0.2545	0.2545	0.1691	0.2569	1.2558	1.5263
2	0.7493	0.8799	0.7416	0.7416	0.7580	0.7580	0.7702	0.7601	1.1590	1.0013
3	-0.0659	-0.1721	-2.0588	-2.0588	-2.0744	-3.0744	-3.0354	-3.0766	-3.0755	-3.2956
4	-0.0659	-0.1721	-2.0588	-2.0588	-2.0744	-3.0744	-3.0354	-3.0766	-3.0755	-3.2956
5	0.5110	0.6064	0.5039	0.5039	1.5189	1.5189	1.4926	1.5209	2.5199	2.7256
6	0.6809	0.7784	1.6737	1.6737	1.6885	1.6885	1.6905	1.6905	2.6894	2.8941
7	0.6809	0.7784	1.6737	1.6737	1.6885	1.6885	1.6905	1.6905	2.6894	2.8941
8	-2.9457	-2.0383	-2.9385	-3.9385	-3.9531	-4.9531	-4.9536	-4.9550	-5.9540	-5.1529
9	63.7	108.7	153.7	198.7	243.7	288.7	333.7	378.7	423.7	468.7
10	-0.1548	-0.2444	-0.1477	-0.1477	-0.1621	-0.1621	-0.1617	-0.1640	-1.1629	-1.3584

Table 11: Multiplicative degree based numerical entropy computation for $MCA.T_n$.

n	EM_1	EM_2	ER	ER_α	EHM	$ESCI_1$	$E\chi_\alpha$	EGA	$EABC$	EH
1	0.5859	0.5485	0.5791	0.5791	1.5926	1.5926	2.5670	2.9532	3.5934	3.5847
2	0.3811	0.3506	0.3760	1.3760	1.3869	2.3869	2.3593	2.5904	3.3878	3.3800
3	-0.9196	-0.3506	-0.9155	-0.9155	-0.9249	-1.9249	-1.8997	-2.0179	-2.9259	-2.9186
4	-0.9196	-0.3506	-0.9155	-0.9155	-0.9249	-1.9249	-1.8997	-2.0179	-2.9259	-2.9186
5	0.3273	0.7303	1.2558	1.9037	2.6741	3.5669	4.5821	5.7198	6.9800	8.3625
6	-0.6719	-0.6479	-0.6686	-0.6686	-0.6766	-1.6766	-1.6540	-1.6165	-1.6775	-1.6711
7	-0.6719	-0.6479	-0.6686	-0.6686	-0.6766	-1.6766	-1.6540	-1.6165	-1.6775	-1.6711
8	-19.1814	-43.8	-76.1	-116.1	-163.7	-219.0	-282.0	-352.6	-430.9	-516.9
9	-0.6282	-0.6071	-0.6257	-0.6257	-0.6323	-0.6323	-0.6122	-1.3949	-1.6332	-1.6276
10	-0.8084	-0.7878	-0.8061	-0.8061	-0.8125	-0.8125	-0.7928	-1.5451	-1.8133	-1.8079

P. N. A. D. Renai *et al.*

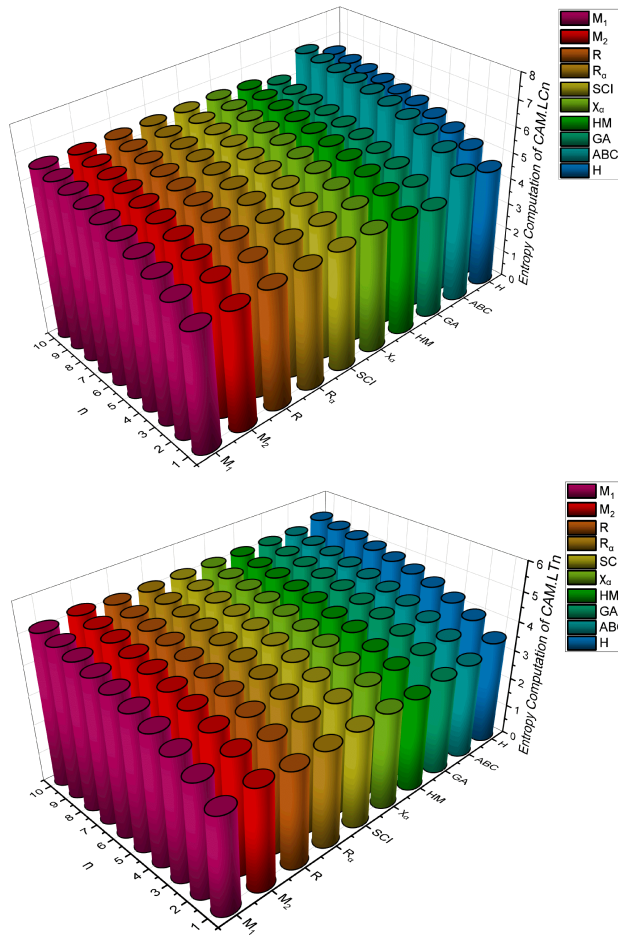*Malaysian J. Math. Sci.* 19(1): 241–267(2025) 241 - 267

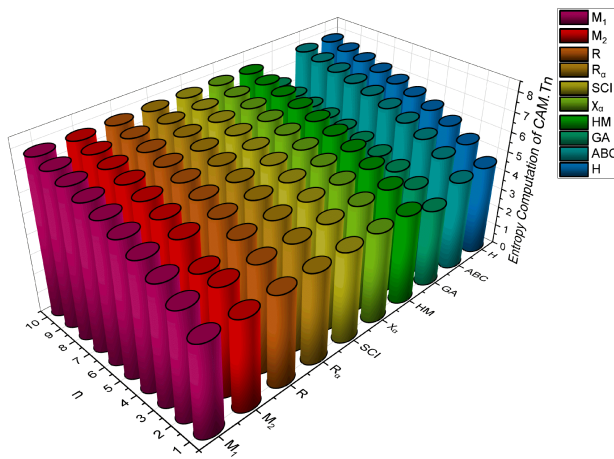Figure 6: Graphical representation of numerical entropy computation for $MCA.LT_n$ and $MCA.LC_n$.

Figure 7: Graphical representation of numerical entropy computation for $MCA.T_n$.

8   Correlation Determination Between Indices and Entropy Values

This section delves into the correlation between specific topological indices, which are based on additive degrees, and the formation of entropy. This concept finds applications across diverse fields such as chemistry, pharmaceuticals, biodrugs, and computer science. By representing these calculated results both visually and numerically, researchers can potentially enhance experimental optimization and time-saving strategies. We conducted calculations for all degree-based entropies across varying values of "n" within three distinct "MCA structures." To facilitate a deeper numerical comparison, specific Tables (6 through 8) outline additive degree-based indices alongside their corresponding entropy formations for smaller "n" values.

Moreover, Figures 7, 8, and 9 provide a scatter plot representation and visual comparisons of these indices and their associated entropy formations within the MCA structures. To elucidate the relationship between variables of differing types, we employed linear regression technique to the data. This methodology allowed us to explore the link between entropy formation and various indices. Utilizing the linear curve fitting method, along with adjustments to underlying parameters, we estimated the alignment between entropy and all indices. Accuracy measures such as standard error estimation, R^2 values, and the linear regression method were leveraged, with a particular focus on R^2 to underscore significance. All simulations were carried out using Microsoft Excel, with Table 12 encapsulating goodness of fit R^2 values for all indices versus entropy.

This table provides numerical evidence of the relationships under scrutiny. This information is invaluable for researchers as it allows them to reduce laboratory work and time consumption by predicting properties based on structural indices, thus guiding experimental design and optimization. Overall, this strategy enables a deeper investigation into the intricate relationships between different types of variables, such as structural indices and thermodynamic properties, facilitating a better understanding of molecular behavior and potential parameter modifications.
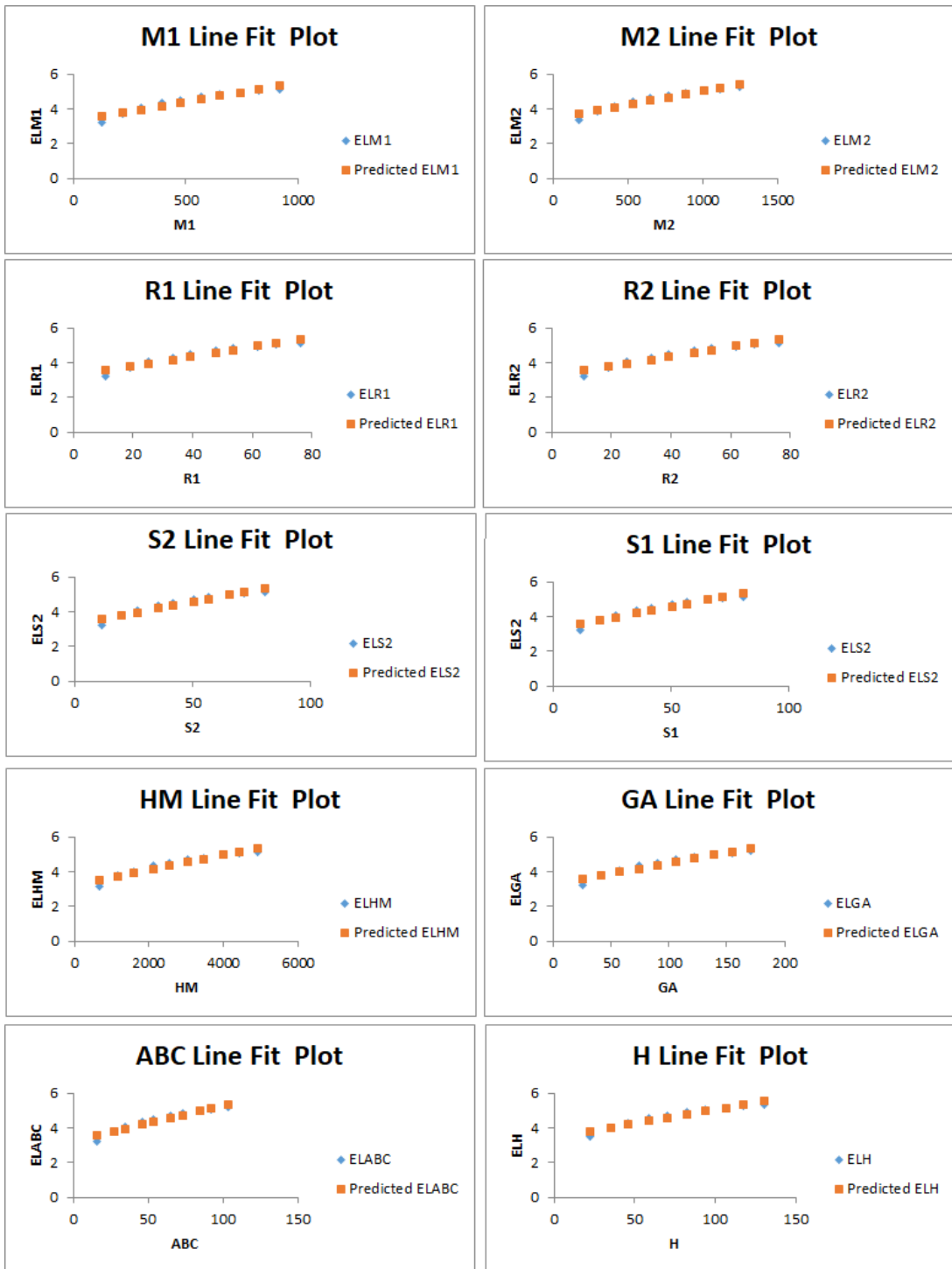
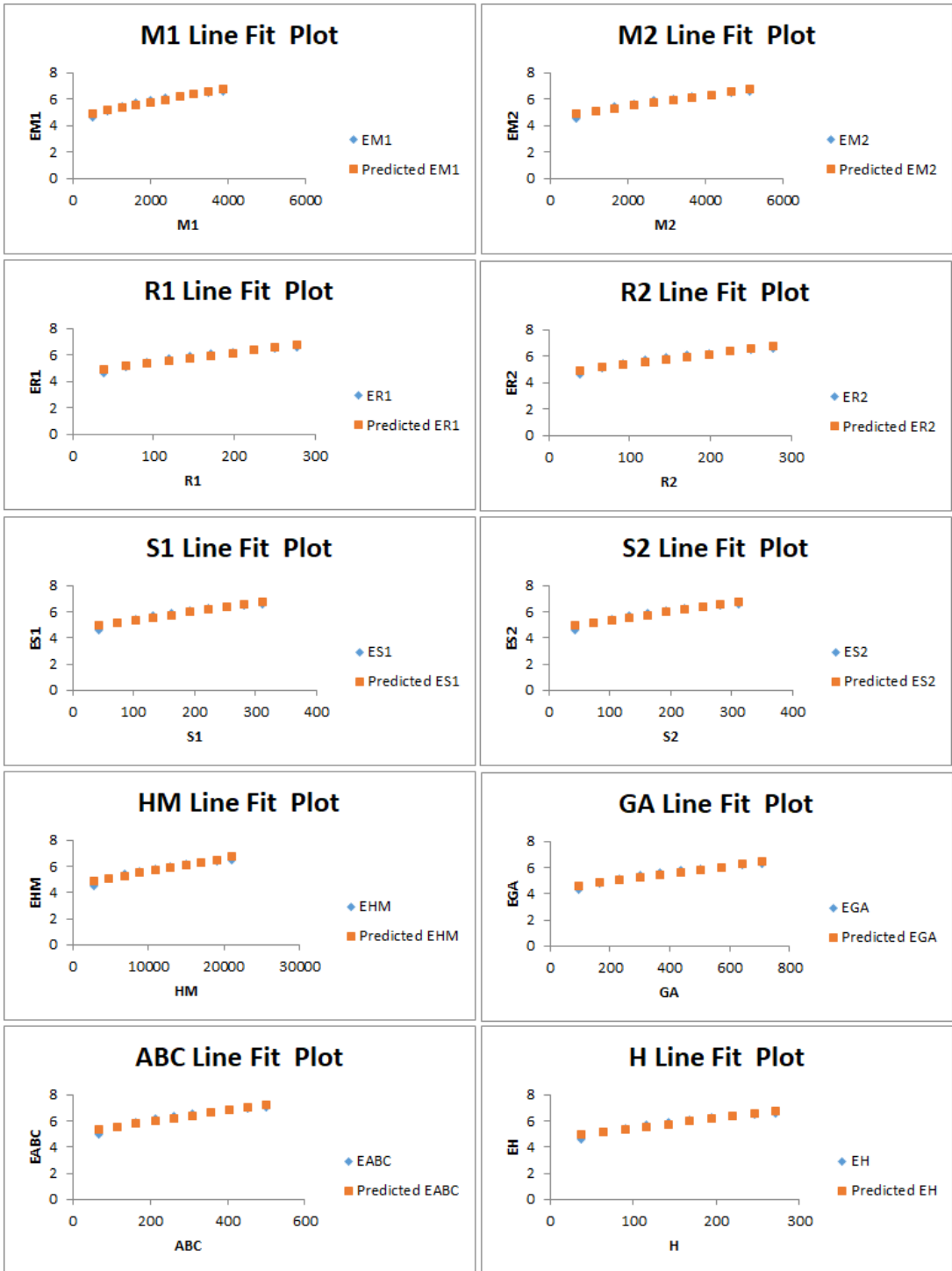Figure 8: Line fitting between indices and entropy values for $MCA.LT_n$.

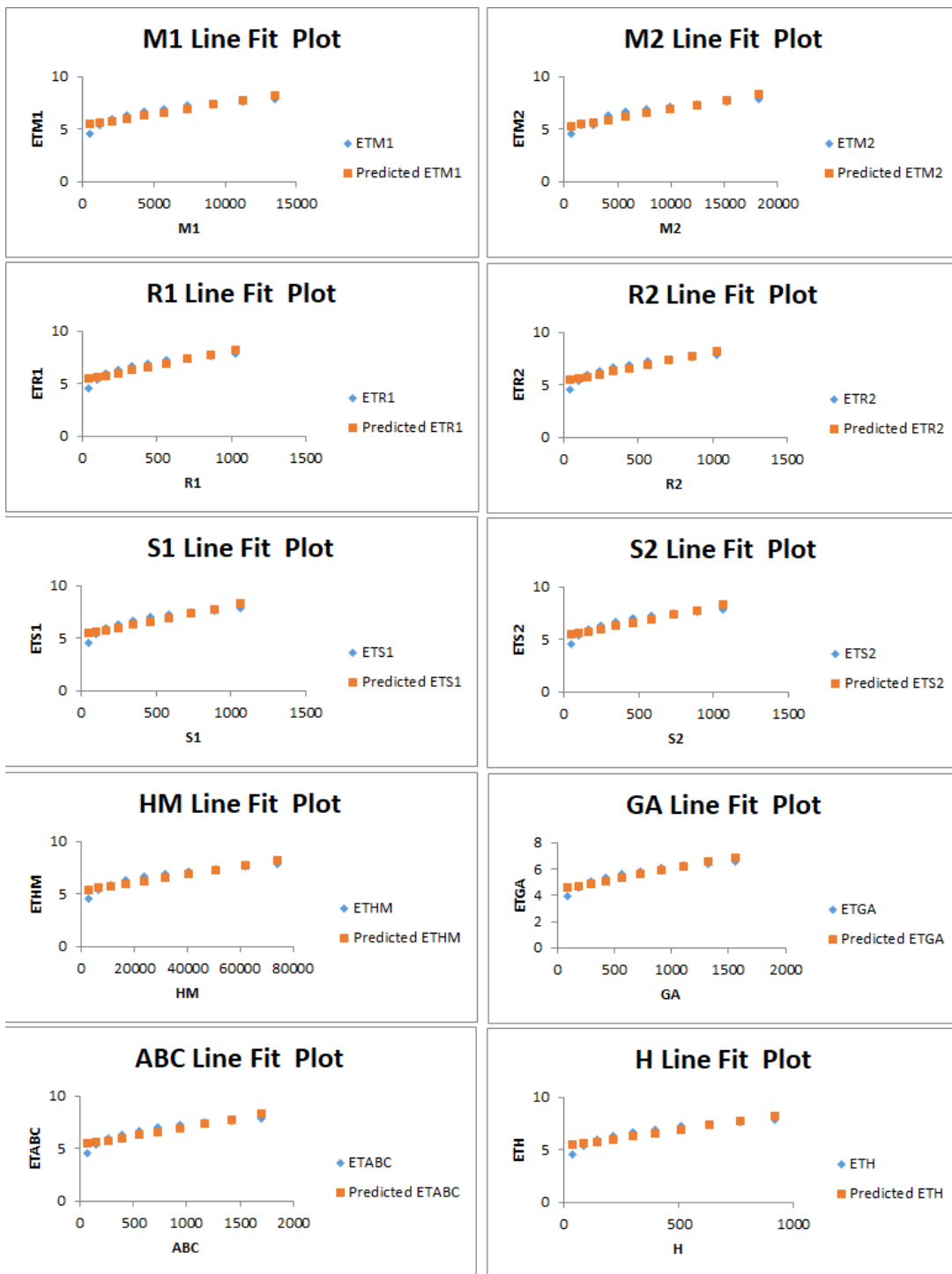Figure 9: Line fitting between indices and entropy values for $MCA.LC_n$.

P. N. A. D. Renai *et al.*

Malaysian J. Math. Sci. 19(1): 241–267(2025) *241 - 267*

Figure 10: Line fitting between indices and entropy values for $MCA.T_n$.

Table 12: Correlation coefficents of $MCA.LT_n$, $MCA.LC_n$ and $MCA.T_n$.

Index	R^2	Standard Error Estimation
M_1	0.96585436	0.168166888
M_2	0.967693977	0.168166888
R	0.9662272	0.184121987
R_α	0.9662272	0.184121987
HM	0.961439715	0.184121987
SCI_1	0.966262737	0.167840131
χ_α	0.966262737	0.167840131
GA	0.965916641	0.16864674
ABC	0.966276259	0.167777467
H	0.968515126	0.155981442

Index	R^2	Standard Error Estimation
M_1	0.963329321	0.182039849
M_2	0.962966136	0.183730085
R	0.963273052	0.182355
R_α	0.963273052	0.182355
HM	0.963383726	0.181776362
SCI_1	0.963383726	0.181776362
χ_α	0.963383726	0.182631626
GA	0.963212808	0.181247402
ABC	0.963495458	0.192579759
H	0.961171366	0.182082957

Index	R^2	Standard Error Estimation
M_1	0.918223504	0.438039746
M_2	0.921370304	0.453220977
R	0.919128362	0.43628526
R_α	0.919128362	0.43628526
HM	0.919164864	0.43527214
SCI_1	0.919164864	0.43527214
χ_α	0.917874771	0.43969581
GA	0.933915731	0.317363205
ABC	0.918949448	0.435824058
H	0.919500595	0.434843906

9   Conclusion

In conclusion, this paper presents an analytical approach for computing information-theoretic entropy in melamine cyanuric acid (MCA) molecular tesselations. Analysis of the three MCA structures revealed that as the n values increase, additive entropy experiences the most significant changes compared to multiplicative entropy. Notably, the Atom Bond Connectivity index consistently delivered optimal incremental outcomes, indicating substantial alterations in disorder during the transition state of MCA. This mathematical methodology, coupled with topological descriptors, provides a comprehensive view of essential thermodynamic parameters, facilitating tailored structural modifications for specific applications. The computed topological indices and entropy metrics for different phases of 2D materials hold promise for predicting a wide range of characteristics such as physicochemical, thermochemical, electrical, and mechanical properties. By integrating these descriptors with quantum-chemical metrics, valuable insights into molecular connectivity and material behavior can be gained. Our exploration highlights the effectiveness of degree-based indices focusing on addition in establishing a correlation between entropy formation and parameter adjustments in MCA compounds, as evidenced by positive correlation coefficients (R^2). Additionally, leveraging Shannon's formula for probabilistic entropy measures establishes links between MCA compound architectures and various physicochemical properties, promising advancements in QSAR and QSPR investigations in this domain.

Conflicts of Interest The authors declare no conflict of interest.

References

[1] M. Arockiaraj, D. Paul, S. Klavžar, J. Clement, S. Tigga & K. Balasubramanian (2022). Relativistic distance based and bond additive topological descriptors of zeolite RHO materials. *Journal of Molecular Structure*, *1250*, Article ID: 131798. https://doi.org/10.1016/j.molstruc.2021.131798.

[2] K. Balasubramanian (2021). Combinatorics, big data, neural network & AI for medicinal chemistry & drug administration. *Letters in Drug Design & Discovery*, *18*(10), 943–948. https://doi.org/10.2174/1570180818666210719130052.

[3] K. Balasubramanian (2022). 2.26 - computational and artificial intelligence techniques for drug discovery and administration. In T. Kenakin (Ed.), *Comprehensive Pharmacology*, pp. 553–616. Elsevier, Oxford. https://doi.org/10.1016/B978-0-12-820472-6.00015-3.

[4] H. A. Baskin. Production of cyanuric acid from urea February 1966. Patent No.: US2363845A.

[5] E. Canelli (1974). Chemical, bacteriological, and toxicological properties of cyanuric acid and chlorinated isocyanurates as applied to swimming pool disinfection: a review. *American Journal of Public Health*, *64*(2), 155–162. https://doi.org/10.2105/ajph.64.2.155.

[6] G. Chehardoli & M. A. Zolfigol (2015). Melamine-$(H_2SO_4)_3$/melamine-$(HNO_3)_3$ instead of H_2SO_4/HNO_3: a safe system for the fast oxidation of thiols and sulfides under solvent-free conditions. *Journal of Sulfur Chemistry*, *36*(6), 606–612. https://doi.org/10.1080/17415993.2015.1074688.

[7] K. S. Chichak, S. J. Cantrill, A. R. Pease, S.-H. Chiu, G. W. V. Cave, J. L. Atwood & J. F. Stoddart (2004). Molecular borromean rings. *Science*, *304*(5675), 1308–1312. https://doi.org/10.1126/science.10969.

[8] M. Cignitti & L. Paoloni (1964). Tautomeric forms of oxy-and oxo-derivatives of 1,3,5-triazine. ii. the ultraviolet absorption of 2,4,6-trimethoxy-1,3,5-triazine and 2,4,6-trioxo-1,3,5-trimethylhexahydrotriazine. *Spectrochimica Acta*, *20*, 211–218.

[9] B. D. Gute, G. Grunwald & S. C. Basak (1999). Prediction of the deral penetration of polycyclic aromatic hydrocarbons (PAHs): a hierarchical qsar approach. *SAR and QSAR in Environmental Research*, *10*(1), 1–15. https://doi.org/10.1080/10629369908039162.

[10] I. Gutman & J. Tošović (2013). Testing the quality of molecular structure descriptors. vertex-degree-based topological indices. *Journal of the Serbian Chemical Society*, *78*(6), 805–810. https://doi.org/10.2298/JSC121002134G.

[11] B. Hasenknopf, J. M. Lehn, B. O. Kneisel, G. Baum & D. Fenske (1996). Self-assembly of a circular double helicate. *Angewandte Chemie International Edition in English*, *35*(16), 1838–1840. https://doi.org/10.1002/anie.199618381.

[12] S. Hassani, F. Tavakoli, M. Amini, F. Kobarfard, A. Nili Ahmadabadi & O. Sabzevari (2013). Occurrence of melamine contamination in powder and liquid milk in market of iran. *Food Additives & Contaminants: Part A*, *30*(3), 413–420. https://doi.org/10.1080/19440049.2012.761730.

[13] A. K. C. Hau, T. H. Kwan & P. K. T. Li (2009). Melamine toxicity and the kidney. *Journal of the American Society of Nephrology*, *20*(2), 245–250. https://doi.org/10.1681/ASN.2008101065.

[14] F. Huang & E. V. Anslyn (2015). Introduction: supramolecular chemistry. *Chemical reviews*, *115*(15), 6999–7000. https://doi.org/10.1021/acs.chemrev.5b00352.

[15] M. N. Husin, R. Hasni & N. E. Arif (2015). Zagreb polynomials of some nanostar dendrimers. *Journal of Computational and Theoretical Nanoscience*, *12*(11), 4297–4300. https://doi.org/10.1166/jctn.2015.4354.

[16] M. Imran, A. R. Khan, M. N. Husin, F. Tchier, M. U. Ghani & S. Hussain (2023). Computation of entropy measures for metal-organic frameworks. *Molecules*, *28*(12), 4726. https://doi.org/10.3390/molecules28124726.

[17] H. F. Ji & X. Xu (2010). Hexagonal organic nanopillar array from the melamine-cyanuric acid complex. *Langmuir*, *26*(7), 4620–4622. https://doi.org/10.1021/la100364v.

[18] S. R. J. Kavitha, J. Abraham, M. Arockiaraj, J. Jency & K. Balasubramanian (2021). Topological characterization and graph entropies of tessellations of kekulene structures: existence of isentropic structures and applications to thermochemistry, nuclear magnetic resonance, and electron spin resonance. *The Journal of Physical Chemistry A*, *125*(36), 8140–8158. https://doi.org/10.1021/acs.jpca.1c06264.

[19] R. Kazemi (2016). Entropy of weighted graphs with the degree-based topological indices as weights. *MATCH Communications in Mathematical and in Computer Chemistry*, *76*(1), 69–80.

[20] A. Modabish, M. N. Husin, A. Q. Alameri, H. Ahmed, M. Alaeiyan, M. R. Farahani & M. Cancan (2022). Enumeration of spanning trees in a chain of diphenylene graphs. *Journal of Discrete Mathematical Sciences and Cryptography*, *25*(1), 241–251. https://doi.org/10.1080/09720529.2022.2038931.

[21] A. Mowshowitz & M. Dehmer (2012). Entropy and the complexity of graphs revisited. *Entropy*, *14*(3), 559–570. https://doi.org/10.3390/e14030559.

[22] M. P. Rahul, J. Clement, J. S. Junias, M. Arockiaraj & K. Balasubramanian (2022). Degree-based entropies of graphene, graphyne and graphdiyne using Shannon's approach. *Journal of Molecular Structure*, *1260*, 132797. https://doi.org/10.1016/j.molstruc.2022.132797.

[23] B. Roy, P. Bairi & A. K. Nandi (2014). Supramolecular assembly of melamine and its derivatives: nanostructures to functional materials. *RSC advances*, *4*(4), 1708–1734. https://doi.org/10.1039/C3RA44524K.

[24] D. S. Sabirov & I. S. Shepelevich (2021). Information entropy in chemistry: An overview. *Entropy*, *23*(10), Article ID: 1240. https://doi.org/10.3390/e23101240.

[25] C. G. Skinner, J. D. Thomas & J. D. Osterloh (2010). Melamine toxicity. *Journal of Medical Toxicology*, *6*, 50–55. https://doi.org/10.1007/s13181-010-0038-1.

[26] S. Taksinoros & H. Murata (2012). Effects of serum proteins on in vitro melamine-cyanurate crystal formation. *Journal of Veterinary Medical Science*, *74*(12), 1569–1573. https://doi.org/10.1292/jvms.12-0138.

[27] J. S. Vijay, S. Roy, B. C. Beromeo, M. N. Husin, T. Augustine, R. Gobithaasan & M. Easuraja (2023). Topological properties and entropy calculations of aluminophosphates. *Mathematics*, *11*(11), Article ID: 2443. https://doi.org/10.3390/math11112443.

[28] V. N. Viswanadhan, G. A. Mueller, S. C. Basak & J. N. Weinstein (2001). Comparison of a neural net-based QSAR algorithm (PCANN) with hologram-and multiple linear regression-based QSAR approaches: application to 1, 4-dihydropyridine-based calcium channel antagonists. *Journal of Chemical Information and Computer Sciences*, *41*(3), 505–511. https://doi.org/10.1021/ci000072+.

[29] Y. Wei & D. Liu (2012). Review of melamine scandal: still a long way ahead. *Toxicology and Industrial Health*, *28*(7), 579–582. https://doi.org/10.1177/0748233711416950.